

Decentralized Reinforcement Learning for Multi-Agent Multi-Resource Allocation via Dynamic Cluster Agreements

Antonio Marino, Esteban Restrepo, Claudio Pacchierotti, Paolo Robuffo Giordano

Abstract—This paper addresses the challenge of allocating heterogeneous resources among multiple agents in a decentralized manner. Our proposed method, LGTC-IPPO, builds upon Independent Proximal Policy Optimization (IPPO) by integrating dynamic cluster consensus, a mechanism that allows agents to form and adapt local sub-teams based on resource demands. This decentralized coordination strategy reduces reliance on global information and enhances scalability. We evaluate LGTC-IPPO against standard multi-agent reinforcement learning baselines and a centralized expert solution across a range of team sizes and resource distributions. Experimental results demonstrate that LGTC-IPPO achieves more stable rewards, better coordination, and robust performance even as the number of agents or resource types increases. Additionally, we illustrate how dynamic clustering enables agents to reallocate resources efficiently also for scenarios with discharging resources.

Index Terms—Distributed Control, Graph Neural Network, Resource Assignment

I. INTRODUCTION

Resource allocation in multi-agent systems (MAS) is a critical challenge across various domains, including robotics, logistics, and disaster management. These tasks require collaborative coordination among agents to address dynamic and heterogeneous demands while adhering to environmental and operational constraints. The inherent complexities of such problems derive from the need for agents to operate in partially observable environments, manage resource heterogeneity, and make decentralized decisions to ensure scalability and robustness [1], [2]. Traditional centralized approaches to resource allocation often become impractical in real-world scenarios due to computational and communication constraints, particularly in large-scale systems [3].

Several studies have proposed distributed solutions to the multi-robot allocation problem. Morgan et al. [4] employed a distributed auction algorithm to allocate agents to predefined locations, forming reconfigurable configurations. Similarly, in [5], the allocation problem was addressed using graph neural networks (GNN), which reduce the information required by individual agents. The authors of [6] formulated the problem as a Markov Decision Process (MDP) to dynamically allocate resources in uncertain environments. Although they demonstrate their scalability to large teams, none of these works consider the heterogeneity of resources and robots.

Using a distributed optimization formulation, the work [7] tackled specifically the heterogeneous allocation problem. In this approach, the overall cost to optimize is expressed as a sum of local losses available to each agent, such as the total motion of robots. However, the general case of resource allocation contains global costs, non-trivially decomposable into local losses. By formalizing the problem as a coverage task with a dynamic density function, the authors of [8] provided a more comprehensive solution that incorporates dynamic resource values and positions. However, the practical implementation of this algorithm suffers from local minima and numerical instability, particularly when only low resource values remain.

An innovative solution has been proposed in [9], where the robot spatial allocation problem is modeled like an opinion dynamics framework. Here, different opinions correspond to distinct consensus clusters. By organizing robot allocations into sub-teams through emergent clusters, this method enables effective and decentralized task distribution among agents. However, its adaptability to dynamic environments is constrained, as agents are required to reset their opinions whenever environmental conditions change, requiring a trigger mechanism to compute the new opinion agreement. Despite this limitation, the concept of dynamic opinion clustering aligns well with multi-resource allocation tasks, where the emergence of subgroup behaviors is essential to simultaneously address and satisfy diverse demands.

Dynamic clustering agreement in network systems has been extensively analyzed during the past years. Giving a team of agents in a connected graph, cluster consensus aims to achieve consensus within subgroups of agents, each containing fewer members than the overall team. In [10], [11] the conditions for the arising of cluster consensus are listed. Besides specific graph topology and negative weighted graphs, other conditions include non-linear and heterogeneous dynamics. The work in [9] falls in the non-linear dynamics category. Another work [12] mixes non-linear and heterogeneous elements imposing bifurcation points to create clustering equilibria. However, devising a general methodology to design the non-linear and heterogeneous dynamics that leads to clustering equilibria remains a challenge.

In this paper we opted to learn this opinion dynamics through multi-agent reinforcement learning (MARL). MARL has emerged as a powerful framework that enables agents to learn cooperative behaviors without relying on centralized control. Frameworks such as decentralized partially observable Markov decision processes (Dec-POMDPs) [13] provide a formal foundation for modeling such problems. However, practical implementation remains challenging due to issues such as non-stationarity, credit assignment, and scalability [14].

A. Marino is with Univ Rennes, CNRS, Inria, IRISA – Rennes, France. E-mail: antonio.marino@irisa.fr

E. Restrepo, C. Pacchierotti and P. Robuffo Giordano are with CNRS, Univ Rennes, Inria, IRISA – Rennes, France. E-mail: {claudio.pacchierotti,prg}@irisa.fr

This work was supported by the ANR-20-CHIA-0017 project “MULTI-SHARED”

Digital Object Identifier (DOI): see top of this page.

Existing solutions often adopt centralized training with decentralized execution (CTDE) paradigm [15], [16], which utilize a global value function to guide agent policies. While effective in many cases, these methods require the definition of a global state and face significant limitations in environments where subgroup dynamics and localized cooperation are crucial. Specifically, they often struggle with credit assignment for individual agents within a team. Alternative methods, such as Value Decomposition Networks (VDN) [17] and QMIX [18], factorize the global reward into individual components but fail to capture localized coordination in multi-objective tasks. More specific solutions for multi-objective MARL, such as [19], propose to maximize the Pareto efficiency using a weighted sum of different objective (demand) values. However, these solutions remain limited in their ability to handle dynamic and heterogeneous resource allocation scenarios.

To address these challenges, we propose a novel decentralized reinforcement learning framework that leverages cluster consensus, specifically tailored for multi-agent, multi-resource allocation problems. Decentralized training has been shown to reduce bias and, in some cases, lower variance in value function estimation [20], making it a promising approach for tackling the complexities of such environments. Specifically, our contributions are as follows:

- **Decentralized RL with Dynamic Cluster Consensus:** We introduce a consensus cluster value function that leverages shared information among agents to address the credit assignment problem effectively. This approach ensures that agents dynamically form clusters to handle subgroup-specific demands while maintaining global coordination.
- **Reward Design for Multi-Objective Optimization:** We propose a hybrid reward structure that balances global incentives, such as reducing overall resource demand, with local rewards that penalize collisions and reward subgroup cooperation. This design bridges the gap between localized decision-making and system-wide optimization.
- **Experimental Validation in Simulation and Hardware:** We validate our approach through extensive simulations and real-world experiments using drones, demonstrating its robustness and efficiency. The results show that our method outperforms state-of-the-art algorithms, such as VDN, QMIX, and Multi-Objective Multi-Agent PPO (MOMAPPO) [8], in terms of resource allocation performance and adaptability.

II. PROBLEM STATEMENT

In this section, we introduce the problem using the markov games formalism, following the reinforcement learning (RL) literature. Consider a resources-assignment task involving a fully cooperative multi-agent team \mathcal{V} composed of N agents operating in a bounded, convex environment $Q \subset \mathbb{R}^n$. The task requires delivering r different resources of different type τ to M consumers located in Q , where each consumer may demand a subset of the available resources. Each consumer has an interaction area R_m , within which an agent's resource can be released to satisfy the demand. We consider two

resource types by their depletion dynamics: 0-depletion, which requires the agents to remain at the location, and instantaneous depletion. We used these two types to represent the two opposite extremes of the depletion dynamics (extremely fast or slow), see Fig. 1.

The system's state $s \in \mathcal{S}$ is defined by the agents' positions $p \in Q$, the consumers' positions $d \in Q$, and the resources associated with the agents' supplies r_p and the consumers' demands r_d . We assume that the sum of the available supplies r_p is less or equal to the sum of r_d . The state evolves according to a transition probability $P(s'|s, u) : \mathcal{S} \times \mathcal{U} \times \mathcal{S} \rightarrow [0, 1]$, where $u \in \mathcal{U}^N$ represents the agents' joint actions. Agents have access to partial observations $z_i \in \mathcal{Z}$, which include only the agent's position p_i , their resources r_{pi} , and all consumer positions d_m and their associated resource demands r_{dm} . Additionally, agents are allowed to communicate with their neighbours $\mathcal{N}_i = \{v_j \in \mathcal{V} \mid \|p_i - p_j\|_2 \leq C, j \neq i\}$, meaning that communication is restricted to a sphere of radius C centered at each agent.

The objective of the task is to find a collaborative control policy that enables the agents to satisfy, at best, the resource demands within the environment. Each agent receives a reward $rw_i(s, u) : \mathcal{S} \times \mathcal{U} \rightarrow \mathbb{R}$ for fulfilling demands. The problem can be formally defined as a Decentralized Partially Observable Markov Decision Process (Dec-POMDP) [13], represented by the tuple

$$\langle \mathcal{S}, \mathcal{U}, P, \{rw_0, \dots, rw_N\}, \mathcal{Z}, \gamma \rangle,$$

where $\gamma \in [0, 1)$ is the discount factor. Under the agent policy distribution $\pi_i(z_i)$, the team performance is defined by the discounted objective function:

$$J_i = \mathbb{E}_{s_0 \sim P_0, s' \sim P, u \sim \pi} \left[\sum_{t=0}^{\infty} \gamma^t rw_i \right]; \quad J = \sum_{i=0}^N J_i. \quad (1)$$

The problem is thus reduced to finding the agent reward rw_i and the optimal policy distribution $\pi_i(z_i)$ that maximize J . Furthermore, the reward rw_i must be carefully designed to account for collective achievements, such as demand satisfaction, while also considering agent motion constraints (e.g., avoiding collisions, staying within the environment boundaries, etc.). Note that the reward rw_i depends on the joint state and actions of all agents, not just on agent i 's state and control.

III. METHOD

To address the problem described in Section II, we implement a MARL strategy. Specifically, we consider that agents must collectively supply resources to fully meet consumer demands, as illustrated in Fig. 1.

A. Reward shaping

While the literature on fully cooperative games in RL often assumes global rewards equally shared among agents [14], we design a combination of local and global rewards. This task requires a balance between global coordination and localized cooperation among smaller groups of agents contributing to resource delivery for the same consumer.

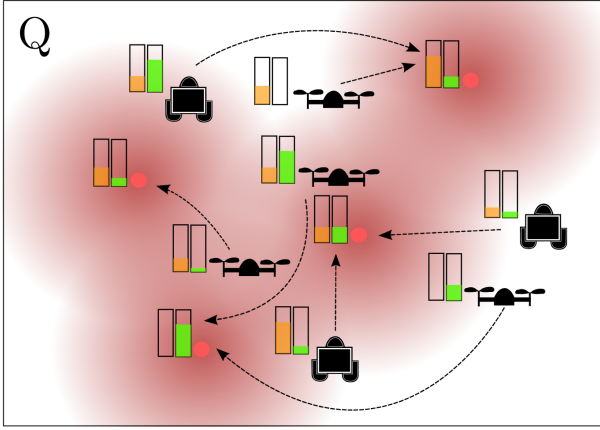


Fig. 1: An assignment example involving a group of heterogeneous robots transporting diverse resources. The robots are allocated to optimally fulfill consumer demands, which are represented by the red dots.

First, we reward the entire team for reducing the overall resource demand:

$$rw_g = \sum_{r_d} \sum_m (r_{md}(t-1) - r_{md}(t)).$$

Additionally, agents receive a global reward if there exists at least one agent releasing resources at every consumer location: $rw_s > 0$. For the local reward, we penalize collisions among agents by introducing a negative reward proportional to the squared distance between agents closer than a threshold ϵ :

$$rw_{ij} = -\gamma_{ij} \|p_i - p_j\|_2^2 \quad \text{if} \quad \|p_i - p_j\|_2^2 < \epsilon, \gamma_{ij} > 0.$$

Agents are rewarded for releasing to the instantaneous depletion resources, with the reward for the agent proportional to the resources released: $rw_{im} > 0$. When the instantaneous consumer demands are fully satisfied, the sub-team contributing to this fulfillment receives an additional reward: $rw_{rc} > 0$. When an agent satisfies a 0-depletion demand, the agent is rewarded with a fixed quantity: $rw_{is} > 0$.

We also introduce a reward to guide agents toward an optimal assignment that minimizes global resource demand. For this purpose, we use a mixed-integer quadratic programming (MIQP) approach to determine the optimal centralized assignment $a \in \mathbb{B}^{N \times M}$ for agents to consumers:

$$\begin{aligned} \min_x \quad & \|r_d - a^T r_p\|_2^2 + (d_{pd} \circ (\sum_{i=0}^r r_{pi} \otimes \mathbf{1}_M) + r_p (\frac{1}{r_d})^T)^T a, \\ \text{s.t.} \quad & \sum_{j=0}^M a_{ij} = 1, \quad \sum_{i=0}^N a_{ij} \geq 1, \quad a \in \{0, 1\}^{N \times M}. \end{aligned} \quad (2)$$

Where the inverse in the second term of the loss ($\frac{1}{r_d}$) has to be intended as element-wise inversion and $\mathbf{1}_M$ is the unitary vector of dimension M . The resulting assignments

from the optimization (a_i) are used to design agent rewards, encouraging agents to align with the correct assignment:

$$rw_{id} = \begin{cases} \|p_i(t-1) - d_{a_i}\|_2^2 - \|p_i(t) - d_{a_i}\|_2^2, & \text{if } p_i(t) \notin R_{a_i}, \\ \gamma_{id} > 0, & \text{if } p_i(t) \in R_{a_i}. \end{cases}$$

Here, R_{a_i} denotes the consumer interaction area. The overall agent reward is the sum of these rewards

$$rw_i = rw_{id} + rw_{is} + rw_{rc} + rw_{im} + \sum_{j=0}^N rw_{ij} + rw_s + rw_g. \quad (3)$$

The local rewards, the group reward rw_{rc} , and the accumulated reward γ_{id} contribute to make the agents' reward similar only if they select the same demanding consumer. Previous approaches using the centralized training with the decentralized execution (CTDE) paradigm, such as MADDPG [16] or COMA [15], do not apply to this reward definition as they struggle to solve the value credit assignment. Moreover, CTDE requires a separate value neural network for each agent with shared information predicting the global value leading to problems like a curse of dimensionality and high variance estimation [20]. Other approaches designed to solve the credit assignment problem for a global shared reward, such as VDN [17] or QMIX [18], are ineffective to capture subgroup rewards, as practically shown in Section IV. We therefore adopted a decentralized training with a decentralized execution (DTDE) leveraging communication to deal with the partial observability of the agents. This allows to keep the value function estimation separated for each agent, training it on the agent reward only. Moreover, we facilitate the training by employing a shared parameter strategy for the neural network architecture described below.

B. Neural network architecture

We deploy two neural networks with the same architecture for the policy and the value function predictions. Given the multi-objective nature of the task, our neural model solution relies upon dynamic cluster consensus that naturally imposes subgroup agreements. Specifically, the demanding consumer features shape the team cluster consensus. In this way, the cluster formation can have a physical meaning for the policy (the agents divide in sub-groups to satisfy the demands) but can also represent the value function clustering, in line with the rewards definition. The current models [21], [12], [22] developed for dynamic clustering either do not allow the dynamic change of the clustering equilibrium or rely on specific graph topology. Therefore, we design a dynamic model that overcomes these limitations.

Firstly, each agent processes the demanding locations and resources using DeepSets [23] as follow:

$$\Phi_m = \phi_2 \left(\sum_{r_{md}} \phi_1(d_m, r_{md}, \tau_{md}) \right). \quad (4)$$

Here, ϕ_1 and ϕ_2 are two multi-layer perceptrons (MLPs) that process and combine the consumer's resource information. Similarly, each agent processes its own resources

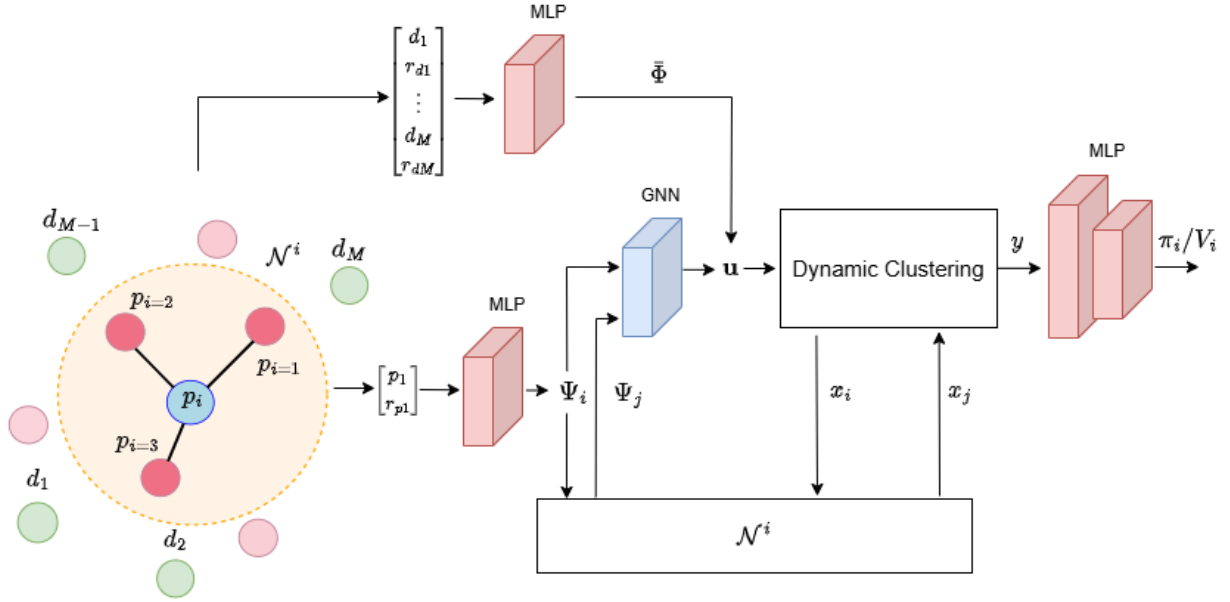


Fig. 2: Neural network model architecture for the value and policy estimation

as $\Psi_i(p_i, r_{p_i}, \tau_{md})$. The consumer features form the feature vector $\Phi = [\Phi_0, \dots, \Phi_M]^T \in \mathbb{R}^{M \times G}$, while the agent features constitute the vector $\Psi = [\Psi_0, \dots, \Psi_N]^T \in \mathbb{R}^{N \times G}$. The agent feature vector Ψ_i is shared among agents using a graph filter and, together with the consumers features, forms the input u as follows:

$$u = \sum_{k=0}^1 S^k \bar{\Psi} \hat{B}_k + \sum_m \Phi_m + b_u. \quad (5)$$

As pointed out in [11], the key elements in the dynamic model for cluster consensus are saturated nonlinearity and heterogeneous dynamics. In this work, we incorporate a continuous-time neural model based on LGTC [24], which inherently possesses saturated dynamics, and introduce a dynamic selector to process the input u , thereby introducing heterogeneous elements among the agent dynamics:

$$\begin{cases} \Xi = \text{softmax} \left(\sigma_c \left(u + \sum_{k=0}^1 S^k x \hat{A}_k + b_x \right) \bar{\Phi}^T \right) \\ f = \rho \left(W \Phi \underset{m \in \{1, \dots, M\}}{\arg \max} \Xi_m + b \right) \\ \dot{x} = -(\tau + f) \circ x - Sx A + f \circ B_f \\ y = [x, \Xi \Phi, u, p] \end{cases} \quad (6)$$

Here, ρ denotes the ReLU activation function, while σ_c is the Tanh activation function. The team state $x \in \mathcal{X} \subseteq \mathbb{R}^{N \times F}$ has F features, and $S \in \mathbb{R}^{N \times N}$ represents the graph's sparsity pattern (e.g., Laplacian or adjacency matrix). The matrices weights \hat{B}_k, \hat{A}_k, A and biases b_x, τ, B_f are learnable parameters. The biases are defined as $1_N \otimes b$, ensuring uniform biases for all agents. The attention coefficients $\Xi \in \mathbb{R}^{N \times M}$ encode the relative importance of consumer features in guiding agent motion, with the maximum coefficient selecting the dominant consumer features that influence the state x . The

attention Ξ depends on the current input but also on the clustering states of the entire team. The output y encapsulates the current state, the weighted sum of the consumers' features, input, and agent positions.

We denote the induced infinity norm as $\|\cdot\|_\infty$ and the induced infinite log-norm $\mu_\infty(\mathbf{X}) = \max_i(x_{ii} + \sum_{j=1, j \neq i}^n |x_{ij}|)$. In the following, we used the vector operator \mathbf{X}_\uparrow that rearranges the elements of matrix \mathbf{X} in a vector. For the filters in system (6), we use the following notation:

$$S_I \triangleq [I, S] \quad \hat{A}_{0,K} \triangleq [\hat{A}_0, \hat{A}_1]^T \quad \hat{B}_{0,1} \triangleq [\hat{B}_0, \hat{B}_1]^T \quad (7)$$

Given the following assumptions

Assumption 1. The bias B_f is unity-bounded: $B_f \subseteq [-1, 1]^{N \times F}$, i.e. $\|B_f\|_\infty \leq 1$,

Assumption 2. Given any two support matrices $\|S_1(t)\|_\infty$ and $\|S_2(t)\|_\infty, \forall t \in \mathbb{R}^+$ associated with two different graphs, they are bounded by the same $\|\tilde{S}\|_\infty$; moreover, they are lower bounded by $\|\tilde{S}\|_\infty$,

we provide the following theorem for the neural ODE (6).

Theorem 1. Under Assumption 1 and 2, with $x(0) \in \mathcal{X}$, system (6) is infinitesimally contractive and the state is bounded in the range $[-1, 1]$, if the following constraints are satisfied

$$\tau \geq 0, \quad \mu_\infty(A^T \otimes S) \geq 0; \quad x(0) \in \mathcal{X} \subseteq [-1, 1]^{N \times G} \quad (8)$$

with the contraction rate

$$c = \mu_\infty(\text{diag}(\tau) + (A^T \otimes \tilde{S}) + \text{diag}(f)) \quad (9)$$

Proof. The proof is available in [24] \square

Remark 1. In practice, we replace A with $A^T A$ and used the left normalized adjacency matrix for S to guarantee the condition $\mu_\infty(A^T \otimes S) \geq 0$ and easily define $\|\tilde{S}\|_\infty, \|\tilde{S}\|_\infty$

Theorem 2. *The distributed system in (6) clusters in different stable equilibrium x_i^c dictated by the demanding dynamics.*

Proof. To prove the statement of the theorem, we need to show that the agents have the same particular state trajectories if they select the same dynamics (therefore if they belong to the same sub-team) and that this particular trajectory is a global attractor for the agents in the sub-team.

There exists N agent state trajectories $[x_0^c, \dots, x_N^c]$ composing the team state vector $\bar{x}^c = \mathbf{1}_N \otimes [x_0^c, \dots, x_N^c]^T$. If the agents belong to the same cluster C_m , they will have the same state trajectories or more formally $\{x_i^c = x_j^c \mid i, j \in C_m, m = [1, \dots, M]\}$ for M different clusters. Let us define the f_{mi} dynamics corresponding to the m -th consumer selected by the agent i as

$$f_{mi} = \rho(W\Phi_m + b).$$

Vector $\bar{f}_M = \mathbf{1}_N \otimes [f_{m1}, \dots, f_{mN}]^T$ consists of the consumer resource dynamics. Therefore the equilibrium trajectories are defined by:

$$\dot{x}_i^c = -\tau \circ x_i^c + f_{mi} \circ (B_f - x_i^c) - S_i \bar{x}^c A \quad (10)$$

with S_i being the i -th row of S . The $\text{ReLU} = \max(\cdot, 0)$ is analyzed in the two cases of the max operator for each element q of the state x_i^c . Therefore, there exist two cases:

$$\begin{cases} \dot{x}_{iq}^c = -\tau_q x_{iq}^c + f_{miq}(B_{fq} - x_{iq}^c) - S_i \bar{x}_q^c A_q \\ \dot{x}_{iq}^c = -\tau_q x_{iq}^c - S_i \bar{x}_q^c A_q \end{cases}.$$

By selecting agent j in the same cluster of i , the difference of their dynamics ($\dot{x}_{iq}^c - \dot{x}_{jq}^c$) is equal to

$$\dot{x}_{iq}^c - \dot{x}_{jq}^c = S_j \bar{x}_q^c A_q - S_i \bar{x}_q^c A_q \quad (11)$$

because they share the same dynamics f_m . The difference in eq(11) is equal to zero only if $S_j \bar{x}_q^c A_q = S_i \bar{x}_q^c A_q$. This condition is satisfied as long as S has constant row sum in the block matrices among the clusters, as demonstrated in [11]. Given the Lipschitz constant l and l_S of the state transition dynamics with respect to f and the graph topology, the state trajectories converge exponentially to the trajectory \bar{x}^c driven by the demanding dynamics \bar{f}_M and S_M graph topology satisfying the constant row sum condition, as the system is contracting, that is,

$$\begin{aligned} \|x(t) - \bar{x}^c(t)\|_\infty &< e^{-ct} \|x(0) - \bar{x}^c(0)\|_\infty \\ &+ \frac{l}{c} (1 - e^{-ct}) \sup_{\tau \in [0, t]} \|f(\tau) - \bar{f}_M(\tau)\|_\infty \\ &+ \frac{l_S}{c} (1 - e^{-ct}) \sup_{\tau \in [0, t]} \|S(\tau) - S_M(\tau)\|_\infty \end{aligned}$$

with c being the contraction rate defined by the Theorem 1. \square

A final MLP is used at the end of the architecture to process the system's output, y .

Remark 2. *As noted in the proof of Theorem 2, the formation of the M clusters is influenced by the graph topology, as the sparse matrix S must maintain a constant row sum within the*

block matrices of adjacent clusters. In practice, even if this condition is relaxed, the agents will still converge to their respective clusters. However, the equilibrium states within each cluster will generally differ, with the differences being bounded and proportional to the variations in row sums among agents within the same cluster.

C. Policy Training

The trainable parameters for the policy and value functions are denoted as θ and ϕ , respectively. The agent's policy distribution is modeled as a normal distribution $\pi(\theta) = \mathcal{N}(\mu(\theta), \sigma(\theta))$, where the mean $\mu(\theta)$ and standard deviation $\sigma(\theta)$ are generated by the proposed architecture.

An independent Proximal Policy Optimization (IPPO) strategy is employed to learn the decentralized policy and value function for each agent. The policy and value losses are defined as follows:

$$J_{\pi_i}(\theta, \theta_k) = \min \left(\frac{\pi_i(z_i, \theta)}{\pi_i(z_i, \theta_k)} A_i^{\pi_i(\cdot, \theta_k)}, g(\epsilon, A_i^{\pi_i(\cdot, \theta_k)}) \right) \quad (12)$$

$$J_{V_i}(\phi) = \left(V_i(\phi) - \left(A_i^{\pi_i(\cdot, \theta_k)} + V_i(\phi_k) \right) \right)^2 \quad (13)$$

Here, $\epsilon > 0$ is a small constant to promote safe exploration, and $A_i^{\pi_i(\cdot, \theta_k)}$ is the advantage function, estimated using Generalized Advantage Estimation (GAE) [25]. To satisfy the contractivity conditions outlined in Theorem 1, we added two regularization terms, $\Pi_V(\phi)$ and $\Pi_\pi(\theta)$, added to the value and policy losses, respectively, as follows:

$$\begin{aligned} J_V &= \mathbb{E}_{(a, z) \sim \mathcal{D}} \left[\sum_i^N J_{V_i} + \alpha \Pi_V \right] \\ J_\pi &= \mathbb{E}_{(a, z) \sim \mathcal{D}} \left[\sum_i^N J_{\pi_i} + \alpha \Pi_\pi \right] \end{aligned} \quad (14)$$

Where the team joint actions and the agents' observations (a, z) are randomly sampled from the replay buffer \mathcal{D} and $\alpha > 0$ is a coefficient to softly enforce the contractivity constraints. The regularization terms are defined as:

$$\Pi = \text{softplus}(c) + \text{softplus}(\tau). \quad (15)$$

IV. EVALUATIONS

We trained the proposed method in a simulated environment with 10 agents and 4 consumer locations, each requiring 2 resources of different types. The resource types, the resource quantities and the agent's initial locations were randomized at each rollout reset. The PyTorch implementation of our algorithm is available at the following link¹. All training and evaluations were conducted on a machine running Ubuntu 22.04. with Intel Core i7-9750H @ 2.60GHz CPU, Nvidia RTX 2080Ti and 32G RAM. The agents are modeled as single integrator dynamics running at 20Hz. At the same rate,

¹the link will be available after the review process for complying with the anonymity policy

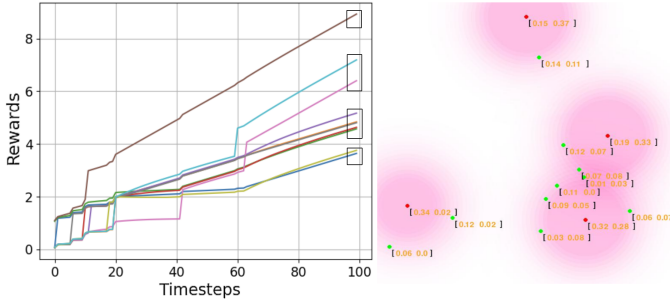


Fig. 3: The agents’ rewards cluster as the agents (green dots) spatially cluster to satisfy the multi-resource demand (red dots)

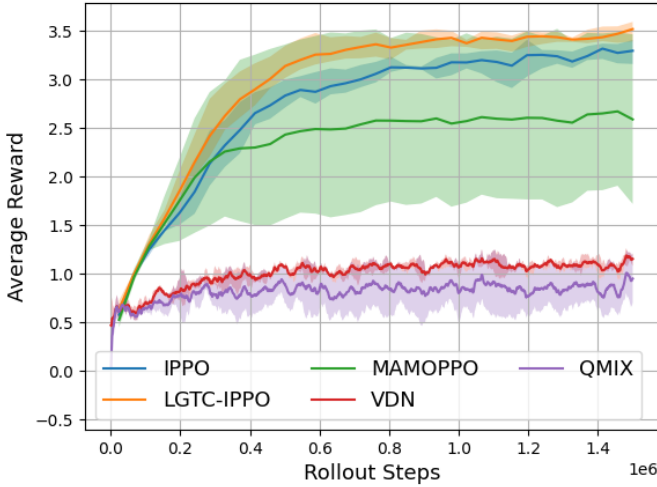


Fig. 4: Mean and standard deviation of accumulated rewards over four training runs with random seeds, reported for our approach and four state-of-the-art MARL methods.

the agents communicate with their neighbours and generate actions from the learned policy. We normalized the agent positions between $[-1, 1]$ and considered a communication range of $C = 1$. in the normalized space.

We want to demonstrate the existence of reward clusters that arise from correct robots’ assignments. Figure 3 presents an assignment case along with the agent’s reward, defined as in Section III-A. As shown, the rewards cluster into similar values for different groups that emerge to complete the task.

We compared our method with Value-Decomposition Networks (VDN) and QMIX to analyze the performance of a decentralized value function versus a global value function. Since the original implementations of VDN and QMIX were designed for discrete action spaces, we adapted these methods by incorporating a soft actor-critic (SAC) [26] strategy. SAC is an off-policy algorithm that uses a soft Q function to maximize policy entropy, aligning with the off-policy nature of VDN and QMIX.

Specifically, denoting the soft Q function for the i -th agent as sQ_i , the soft Q function updates for VDN and QMIX are

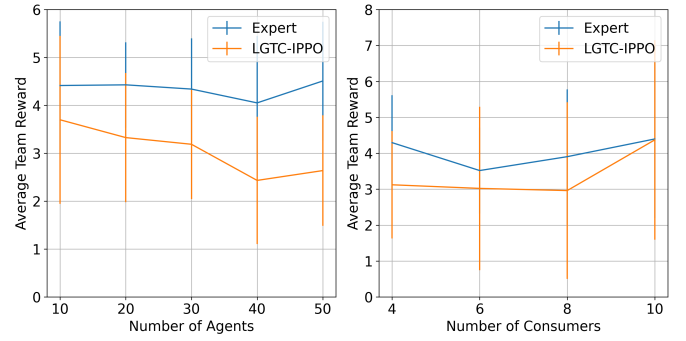


Fig. 5: Mean and standard deviation of accumulated rewards over a variable number of agents and consumers, reported for a centralized expert and our approach (LGTC-IPPO).

Parameters	MOMAPPO/IPPO/LGTC-IPPO	VDN/QMIX
γ	0.99	0.99
λ_{GAE}	0.95	-
batch size	64	256
epochs	4	1
rollout/Replay buffer	6144	20000
entropy coefficient	-	0.01
ϵ	0.2	-
max gradient norm	0.5	0.5
polyak τ	-	0.005
G	64	64
F	64	64
final MLP	[256,256]	[256,256]
MIX	-	[32,32]
adam learning rate	2×10^{-4}	2×10^{-4}

TABLE I: Training parameters

computed as follows:

$$\begin{aligned}
 J_{QVDN}(\phi) &= \mathbb{E}_{(a,z) \sim \mathcal{D}} \left[\left(\sum_i^N Q_i(z_i, a_i, \phi) - rw(s, a) \right. \right. \\
 &\quad \left. \left. - \gamma \mathbb{E}_{z'_i \sim s'_i} \left[\mathbb{E}_{a'_i \sim \pi(\cdot, \theta)} \left[\sum_i^N sQ_i(z'_i, a'_i, \phi) \right] \right] \right)^2 \right], \\
 J_{QMIX}(\phi) &= \mathbb{E}_{(a,z) \sim \mathcal{D}} \left[\left(\text{MIX}(Q_i(z_i, a_i, \phi)) - rw(s, a) \right. \right. \\
 &\quad \left. \left. - \gamma \mathbb{E}_{z'_i \sim s'_i} \left[\mathbb{E}_{a'_i \sim \pi(\cdot, \theta)} \left[\text{MIX}(sQ_i(z'_i, a'_i, \phi)) \right] \right] \right)^2 \right].
 \end{aligned}$$

Here, MIX represents a neural network that combines the individual agent Q functions into a global Q function.

We also benchmark our method against a vanilla IPPO variant, which excludes both the cluster consensus mechanism and loss regularization. For these three methods, we used a policy neural network architecture similar to the proposed method but excluded the dynamic cluster consensus dynamics. Instead, we retained only the consumer feature selection, input features, and agent positions, represented as:

$$y = [(\Xi \circ \Phi)_{\arg \max_{m \in \{1, \dots, M\}} \Xi_{im}, u, p}].$$

However, for these algorithms, the attention Ξ depends on the current input. Additionally, we compared our approach with Multi-Agent Multi-Objective PPO (MAMOPPO) [19], a prominent solution for multi-objective multi-agent problems. This algorithm uses a weighted sum of resources feature to predict the value and policy. Therefore, we use our architecture but we remove the dynamic clustering consensus and the state from the vector y . The Table I summarizes the training parameters.

Figure 4 compares the performance of the different algorithms across multiple random seeds. We named our solution LGTC-IPPO. Our solution achieves the highest mean reward with a low standard deviation of approximately 0.2 by the end of training. As expected, VDN and QMIX quickly stop improving due to the local nature of the rewards. MAMOPPO and IPPO perform closer to our approach, though MAMOPPO exhibits high variance. This is due to the weighted average of consumer features which can sometimes provide a good estimate of the final rewards but fails in the general case. IPPO, which shares the same neural network as our method, performs worse due to its lack of coordination in consumer selection, as it does not incorporate cluster consensus.

Additionally, we compare our solution with an expert centralized approach while varying the number of agents and resources. The centralized controller employs the optimization in Eq.(2) to assign the optimal resource to each agent and uses a proportional controller with centralized obstacle avoidance to guide agents toward their assigned locations while preventing collisions. Figure 5 presents the average team reward for our proposed algorithm (LGTC-IPPO) compared to an expert centralized solution, as the number of agents (left) and the number of consumers (right) vary. The expert consistently outperforms LGTC-IPPO, maintaining a higher reward across different scenarios, as expected, since it uses perfect information about the environment. As the number of agents increases, both methods show a slight decline in performance, but LGTC-IPPO experiences a more pronounced drop. While the expert remains relatively stable around 4–4.5, LGTC-IPPO’s reward decreases significantly, falling below 3 when the number of agents exceeds 30. This suggests that handling conflicts between resource allocation and collision avoidance becomes increasingly challenging for the decentralized approach in crowded environments. On the other hand, varying the number of consumers, the expert maintains a relatively stable reward, while LGTC-IPPO remains consistently lower but follows a similar pattern. Interestingly, for a high number of consumers (10), LGTC-IPPO reaches the expert’s performance, albeit with high variance. This suggests that when more consumers are available, the decentralized approach has more opportunities to make effective decisions, reducing the negative impact of local information limitations.

V. EXPERIMENTS

We evaluated the policy using 5 Crazyflie drones, each loaded with up to 3 mixed resource types. The policy was executed on a central workstation, which transmitted velocity commands to the drones via a radio dongle. The hardware

implementation also incorporated a local Control Barrier Function (CBF) safety filter. The CBF tracks the generated velocity command and adjusts it as necessary to consider a safety distance among the drones. This helps in mitigating the impact of the airflow disturbances caused by other drones on the dynamics of an individual drone. Videos of the experiments are provided in the supplementary materials. Resources requiring instantaneous depletion are colored in green, while resources with 0-depletion requirements are displayed in orange. The physical experiments validated the resource assignment performance observed in the previous section.

To further analyze the system, we focused on a scenario where each drone was assigned a single 0-depletion resource. This resource represented a dischargeable entity critical to the drone’s operation, such as battery level. This setup allowed us to study the equilibrium changes in the dynamic cluster consensus process. Key moments of this scenario are shown in Fig. 6. Initially, after takeoff, the drones allocate their resources to target locations to minimize the remaining demand. At 55 s, we manually reduce the resource level of one drone to simulate the battery discharge process. This causes the drone to land, triggering a reallocation process. To compensate for the absence of the landed drone, another drone is assigned to a new target location, completing the new allocation by approximately 90 s. The value function dynamic states of the 5 drones, shown in Fig. 7 as a normalized projection on the unitary vector, illustrate the system’s response. When the resource (battery) of one drone was depleted, a new set of clustering equilibria emerged, forming clusters that corresponded to the updated resource allocation solution.

VI. CONCLUSION

In this work, we presented LGTC-IPPO, a decentralized reinforcement learning approach for multi-agent multi-resource allocation, incorporating cluster consensus to enhance coordination. By extending IPPO with localized consensus mechanisms, our method improves task allocation efficiency while effectively handling the challenges posed by group rewards. Through extensive evaluations, we demonstrated that LGTC-IPPO outperforms standard MARL baselines in terms of reward stability and coordination. Additionally, our results show that clustering equilibria facilitate agent reallocation when required by changes in consumer demand or team dynamics. Overall, the results show that while centralized approaches still have an advantage in scenarios where full information is available, LGTC-IPPO offers an alternative for environments where such global coordination is either infeasible or too costly.

For the future, we plan to refine the theoretical aspects of dynamic cluster consensus, focusing on its convergence properties in the face of variable communication topologies and stochastic disturbances. Moreover, exploring structured communication protocols and hierarchical planning strategies could further enhance the scalability of our framework. Ultimately, our goal is to extend the applicability of LGTC-IPPO to more complex, real-world scenarios, advancing the state of the art in decentralized multi-agent coordination.

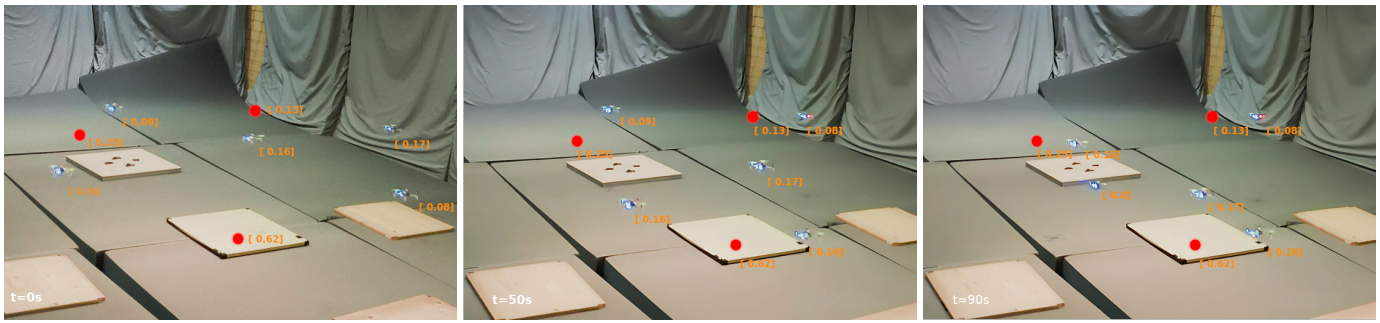


Fig. 6: Dynamic agent reallocation with discharging resources. 5 drones relocate in the space to interact with 3 task locations (red dots). The battery level required by each task and available on each drone is depicted in orange. At 50 s, one drone discharges and lands on the ground, therefore a drone of another subteam relocates to the task left uncovered.

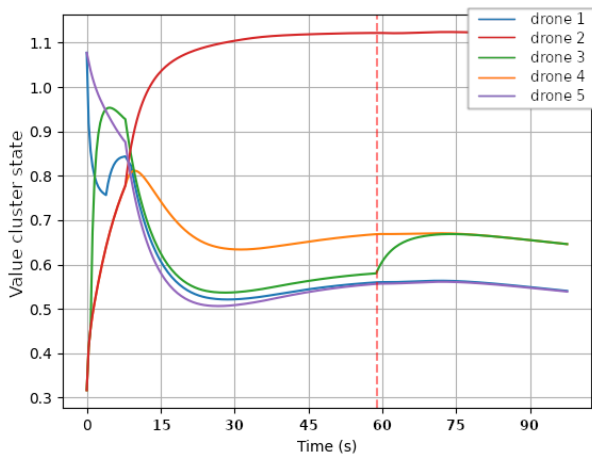


Fig. 7: Dynamic state cluster consensus for the resource discharging case. At the time 50 s, the resource available to drone 3 discharges and drone 4 changes cluster to cover the consumer unsatisfied.

REFERENCES

- [1] A. Khamis, A. Hussein, and A. Elmogy, "Multi-robot task allocation: A review of the state-of-the-art," *Cooperative robots and sensor networks 2015*, pp. 31–51, 2015.
- [2] S. Park, Y. D. Zhong, and N. E. Leonard, "Multi-robot task allocation games in dynamically changing environments," in *2021 IEEE International Conference on Robotics and Automation (ICRA)*. IEEE, 2021, pp. 8678–8684.
- [3] M. Doostmohammadian, A. Aghasi, M. Pirani, E. Nekouei, H. Zarrabi, R. Keypour, A. I. Rikos, and K. H. Johansson, "Survey of distributed algorithms for resource allocation over multi-agent systems," *Annual Reviews in Control*, vol. 59, p. 100983, 2025.
- [4] D. Morgan, G. P. Subramanian, S.-J. Chung, and F. Y. Hadaegh, "Swarm assignment and trajectory optimization using variable-swarm, distributed auction assignment and sequential convex programming," *The International Journal of Robotics Research*, vol. 35, no. 10, pp. 1261–1285, 2016.
- [5] M. Goarin and G. Loianno, "Graph neural network for decentralized multi-robot goal assignment," *IEEE Robotics and Automation Letters*, 2024.
- [6] J. D. Griffith, M. J. Kochenderfer, R. J. Moss, V. V. Mišić, V. Gupta, and D. Bertsimas, "Automated dynamic resource allocation for wildfire suppression," *Lincoln Laboratory Journal*, vol. 22, no. 2, pp. 38–59, 2017.
- [7] A. Camisa, A. Testa, and G. Notarstefano, "Multi-robot pickup and delivery via distributed resource allocation," *IEEE Transactions on Robotics*, vol. 39, no. 2, pp. 1106–1118, 2022.
- [8] M. Coffey and A. Pierson, "Covering dynamic demand with multi-resource heterogeneous teams," in *2023 IEEE/RSJ International Conference on Intelligent Robots and Systems (IROS)*. IEEE, 2023, pp. 11 127–11 134.
- [9] Z. Zhang, W. Wu, and F. Zhang, "Opinion-based task allocation strategy for mobile sensor networks," in *2024 American Control Conference (ACC)*. IEEE, 2024, pp. 123–128.
- [10] F. Sorrentino, L. M. Pecora, A. M. Hagerstrom, T. E. Murphy, and R. Roy, "Complete characterization of the stability of cluster synchronization in complex dynamical networks," *Science advances*, vol. 2, no. 4, p. e1501737, 2016.
- [11] W. Xia and M. Cao, "Clustering in diffusively coupled networks," *Automatica*, vol. 47, no. 11, pp. 2395–2405, 2011.
- [12] A. Bizyaeva, A. Franci, and N. E. Leonard, "Nonlinear opinion dynamics with tunable sensitivity," *IEEE Transactions on Automatic Control*, vol. 68, no. 3, pp. 1415–1430, 2022.
- [13] F. A. Oliehoek, C. Amato *et al.*, *A concise introduction to decentralized POMDPs*. Springer, 2016, vol. 1.
- [14] S. Gronauer and K. Diepold, "Multi-agent deep reinforcement learning: a survey," *Artificial Intelligence Review*, vol. 55, no. 2, pp. 895–943, 2022.
- [15] J. Foerster, G. Farquhar, T. Afouras, N. Nardelli, and S. Whiteson, "Counterfactual multi-agent policy gradients," in *Proceedings of the AAAI conference on artificial intelligence*, vol. 32, no. 1, 2018.
- [16] R. Lowe, Y. I. Wu, A. Tamar, J. Harb, O. Pieter Abbeel, and I. Mordatch, "Multi-agent actor-critic for mixed cooperative-competitive environments," *Advances in neural information processing systems*, vol. 30, 2017.
- [17] P. Sunehag, G. Lever, A. Gruslly, W. M. Czarnecki, V. Zambaldi, M. Jaderberg, M. Lanctot, N. Sonnerat, J. Z. Leibo, K. Tuyls *et al.*, "Value-decomposition networks for cooperative multi-agent learning based on team reward," in *Proceedings of the 17th International Conference on Autonomous Agents and MultiAgent Systems*, 2018, pp. 2085–2087.
- [18] T. Rashid, M. Samvelyan, C. S. De Witt, G. Farquhar, J. Foerster, and S. Whiteson, "Monotonic value function factorisation for deep multi-agent reinforcement learning," *Journal of Machine Learning Research*, vol. 21, no. 178, pp. 1–51, 2020.
- [19] F. Felten, U. Ucak, H. Azmani, G. Peng, W. Röpke, H. Baier, P. Mannion, D. M. Roijers, J. K. Terry, E.-G. Talbi *et al.*, "Momoland: A set of benchmarks for multi-objective multi-agent reinforcement learning," *arXiv preprint arXiv:2407.16312*, 2024.
- [20] X. Lyu, Y. Xiao, B. Daley, and C. Amato, "Contrasting centralized and decentralized critics in multi-agent reinforcement learning," in *Proceedings of the 20th International Conference on Autonomous Agents and MultiAgent Systems*, 2021, pp. 844–852.
- [21] B. Lian, A. T. Korus, W. Xue, F. L. Lewis, and A. Davoudi, "Distributed dynamic clustering and consensus in multi-agent systems," *IEEE Transactions on Automatic Control*, 2024.
- [22] Z. Zhang, S. Al-Abri, and F. Zhang, "A generalized kuramoto model for opinion dynamics on the unit sphere," *Automatica*, vol. 171, p. 111957, 2025.
- [23] M. Zaheer, S. Kottur, S. Ravanbakhsh, B. Poczos, R. R. Salakhutdinov, and A. J. Smola, "Deep sets," *Advances in neural information processing systems*, vol. 30, 2017.

- [24] A. Marino, C. Pacchierotti, and P. Robuffo Giordano, “Liquid-Graph Time-Constant Network for Multi-Agent Systems Control,” in *CDC 2024 - 63rd IEEE Conference on Decision and Control*. Milan (Italie), Italy: IEEE, Dec. 2024.
- [25] J. Schulman, P. Moritz, S. Levine, M. Jordan, and P. Abbeel, “High-dimensional continuous control using generalized advantage estimation,” *arXiv preprint arXiv:1506.02438*, 2015.
- [26] T. Haarnoja, A. Zhou, P. Abbeel, and S. Levine, “Soft actor-critic: Off-policy maximum entropy deep reinforcement learning with a stochastic actor,” in *International conference on machine learning*. PMLR, 2018, pp. 1861–1870.